ORNL/TM-2013/99

Field Testing of Low-Cost Bio-Based Phase Change Materials as Energy Storage Medium in Building Envelopes

March 2013

Prepared by
Kaushik Biswas, Ph.D.
Phillip Childs
Jerald Atchley

ORNL/TM-2013/99

Energy and Transportation Science Division

FIELD TESTING OF LOW-COST BIO-BASED PHASE CHANGE MATERIALS AS ENERGY STORAGE MEDIUM IN BUILDING ENVELOPES

Kaushik Biswas
Phillip Childs
Jerald Atchley

Date Published: March, 2013

Prepared by
OAK RIDGE NATIONAL LABORATORY
Oak Ridge, Tennessee 37831-6283
managed by
UT-BATTELLE, LLC
for the
U.S. DEPARTMENT OF ENERGY
under contract DE-AC05-00OR227

TABLE OF CONTENTS

ABSTRACT

A test wall built with phase change material (PCM)-enhanced loose-fill cavity insulation was monitored for a period of about a year in the warm-humid climate of Charleston, South Carolina. The test wall was divided into various sections, one of which contained only loose-fill insulation and served as a control for comparing and evaluating the wall sections with the PCM-enhanced insulation. This report summarizes the findings of the field test.

1. INTRODUCTION

This project was initiated in 2010 by Syntroleum Corporation, in response to a funding opportunity announcement by the U.S. Department of Energy. The major goal was to fundamentally change the manufacture of phase change material (PCM). The proposed low cost process involves a sustainable and more selective route to PCM paraffins and a low cost approach to converting the paraffins to form-stable PCM pellets. By significantly lowering the payback time for PCM-enhanced building material (e.g. wallboards and insulation), high market penetration and proportionally large environmental benefit is expected.

PCMs in building envelopes operate by changing phase from solid to liquid while absorbing heat from the outside and thus reducing the heat flow into the building, and releasing the absorbed heat when it gets cold outside reducing the heat loss through the building envelope. The energy saving potential of PCMs for buildings has been demonstrated [1], but the traditionally high PCM prices have precluded extensive application of PCMs in the building industry. Commercializing a low cost PCM platform was the main goal of this project. The low cost PCM production process involves two components: (1) on-purpose production of C_{16}-C_{18} paraffins from low cost bio-renewable feedstocks, and (2) low cost encapsulation using under-water pelletizers. Paraffins are straight chain saturated hydrocarbons with high latent heat. Hexadecane ($C_{16}H_{34}$), heptadecane ($C_{17}H_{36}$), and octadecane ($C_{18}H_{38}$) are three paraffins that melt/freeze between 18 ºC (64 ºF) and 28 ºC (82 ºF). This temperature range is considered the comfort zone for most people. The high latent heat and suitable phase change temperature range make these paraffins attractive as PCMs for building applications.

Animal fats and vegetable oils are 97% or higher C_{16} and C_{18} fatty acids, and can be converted to C_{16}-C_{18} paraffins using a reaction called hydrodeoxygenation. Further, studies have shown that paraffins can be trapped into high density polyethylene (HDPE) by co-crystallizing a paraffin/HDPE melt. Up to 70% paraffin can be trapped in the HDPE matrix such that molten paraffin does not seep out solid HDPE matrix. Under-water pelletizers have been successfully used to convert molten polymer systems to pellets of various sizes, including < 1 mm pellets. The combination of C_{16}-C_{18} paraffin production from low value fats and waste vegetable oils, combined with low cost encapsulation via under-water pelletizers, is expected to result in a step-change in PCM production costs.

Syntroleum collaborated with Oak Ridge National Laboratory to field-test their PCMs in one of ORNL's test facilities located in Charleston, SC. The test was initiated in January 2012 for a period of about 1 year. A test was built and installed with different combinations of cellulose and PCM containing HDPE pellets as cavity insulation. The wall was instrumented with

temperature, humidity and heat flux sensors. The data were remotely monitored and downloaded on a weekly basis. All test data were periodically provided to Syntroleum and are being used for whole building modeling to determine the impact of PCM on annual building energy use. This report provides the test wall and sensor details and briefly summarizes the test data, with a description of key findings.

2. TEST FACILITY AND TEST WALL DETAILS

The Syntroleum wall test is ongoing in a Natural Exposure Test (NET) facility in Charleston, SC, shown in Figure 1. NET facilities expose side-by-side roof/attic and wall assemblies to natural weathering in four different humid US climates. The data help industry develop products to avoid adverse moisture-related impacts in buildings, and are essential in validating hygrothermal and energy models. NET structures are located at ORNL and at Charleston, SC; Tacoma, WA; and Syracuse, NY. Each is temperature and humidity controlled and instrumented to measure moisture content in materials, vapor pressure, temperature, heat flux, humidity, etc. Figure 1 shows the southeast wall of the Charleston NET facility, which houses multiple side-by-side test walls. Also shown is a weather station on the southwest gable end of the building.

Figure 1. Charleston, SC NET facility.

Originally, the test wall was constructed in January 2012, followed by a modification in June 2012. Figure 2 shows the test wall frame built for the January installation. It shows three wall cavities, with sensors installed in the center, and separated by wood studs and thin foam insulation strips, along with a retaining net for holding the insulation. The foam strips were added to minimize the thermal interactions between the cavities. The larger cavity was filled with the cellulose-PCM mixture, while one of the smaller cavities was filled with only cellulose insulation to serve as control for comparison and evaluation of the PCM-enhance insulation. The third cavity was filled with a mix of cellulose and HDPE pellets (without PCM), to try and further isolate the effects of PCM on the insulation properties.

The wall was built using 2 x 6 wood studs, resulting in a cavity depth of 14 cm (5.5 inch), with

1.2 cm (0.5 inch) oriented strand board (OSB) attached to the exterior side of the wall. The larger cavity dimensions were 2.2 x 0.4 m^2 (87.8 x 14.5 square inch) and smaller cavities were 1.1 x 0.4 m^2 (42.4 x 14.5 square inch). The nominal amount of PCM in the larger cavity was 20% by weight. The PCM-HDPE pellet design was such that the pellets contained 65% paraffin by weight. Thus, the PCM pellets and cellulose were mixed so that the mixture contained 31% of pellets, or 0.45 kg of pellets for each kg of cellulose. For the cavity with cellulose mixed with the HDPE pellets without PCM, the same volume ratio as the cellulose-PCM pellet mixture was maintained.

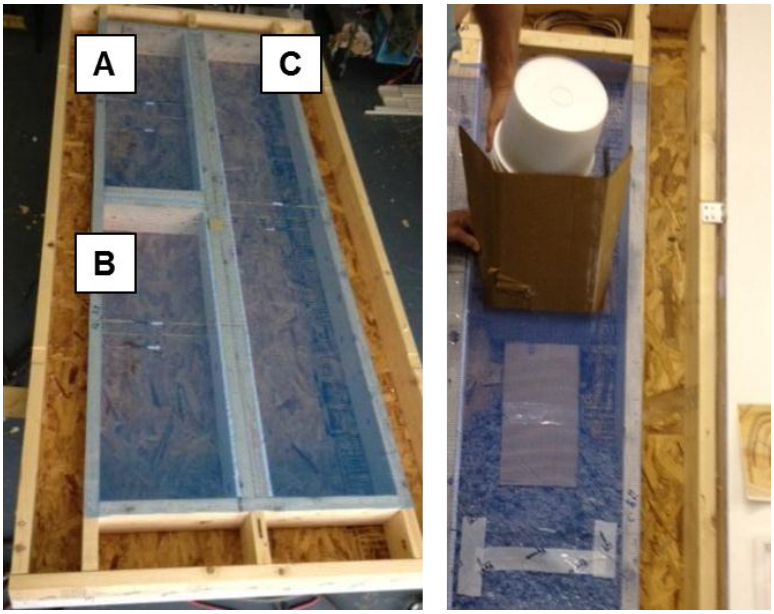

Figure 2. Original test wall frame (January 2012) (left) - (A) cellulose-only insulation, (B) cellulose-HDPE mix, (C) cellulose-PCM mix; Addition of PCM containing insulation to a wall cavity (right).

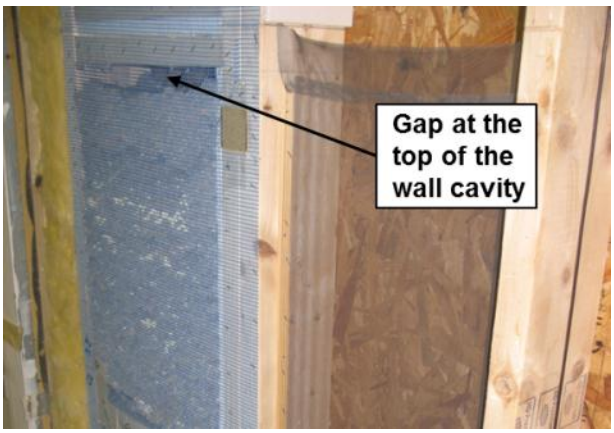

Figure 3. Gap at the top of a cavity.

The cellulose and PCM pellets, in the appropriate ratio, were mixed together in buckets. The wall cavities were loaded by filling insulation through slots cut in the retaining net, also shown in Figure 2, and allowing it to settle under gravity. It should be noted that, after filling, there was further settling of the cellulose insulation in the cavities, which resulted in about 2.5-3.8 cm (1-

1.5 inch) gaps at the top of the cavities with time. This phenomenon was noted when the wall was revisited in June 2012, as shown in Figure 3.

During June, the wall was modified by breaking the larger cavity into two smaller ones, so all the cavities had dimensions of 1.1 x 0.4 m^2 (42.4 x 14.5 square inch). Both the newer cavities contained PCM pellets; however, in one cavity the pellets were mixed in the desired weight ratio with cellulose insulation, while the second one contained a sandwich structure. Figure 4 shows the cellulose-PCM-cellulose sandwich configuration used in one of the additional smaller wall cavities. The second new smaller cavity was filled with a cellulose-PCM mixture containing PCM with different phase change characteristics than the one used in the original cellulose-PCM mix used previously. The newer PCM pellets contained 66% paraffin by weight, which resulted in 30% pellets by weight in the cellulose-PCM mixture. The in-situ density of the newer cellulose-PCM mixture was 61.6 kg/m^3 (3.85 lb/ft^3). The density of the original cellulose-PCM used during the January installation is not available.

Once installed, the outer cavities of the test wall were filled with fiberglass insulation to thermally insulate the wall from the other neighboring test walls, as shown in Figure 5. Further, the gaps observed at the top of the cavities were filled with more cellulose insulation. Figure 6 shows the finished interior and exterior faces of the test wall. The interior side was covered with 1.3 cm (0.5 in) gypsum board and the exterior OSB was covered with a weather resistive barrier (0.15 mm thick high density polyethylene sheet) underneath vinyl siding. Also visible on the interior face are four (4) temperature sensors, one centered on each cavity, which are further described in the next section.

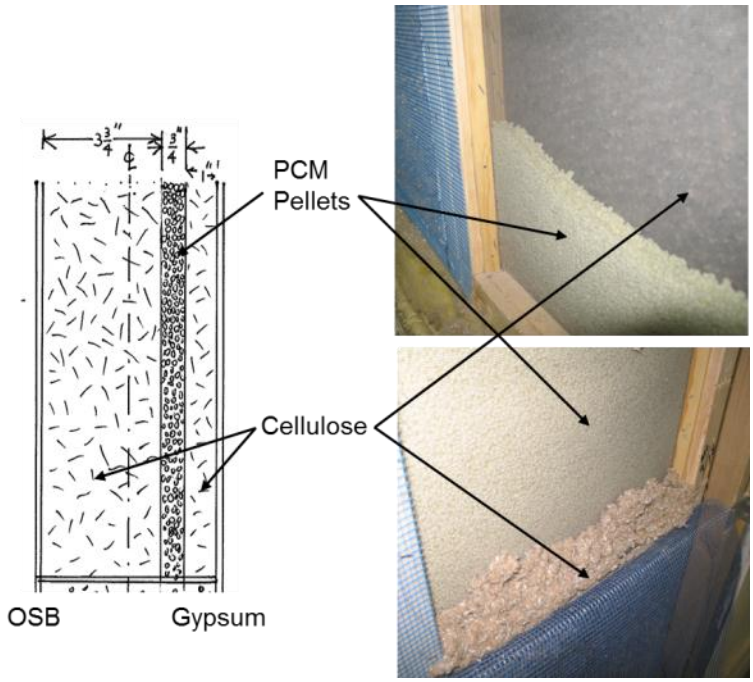

Figure 4. Cellulose-PCM sandwich structure.

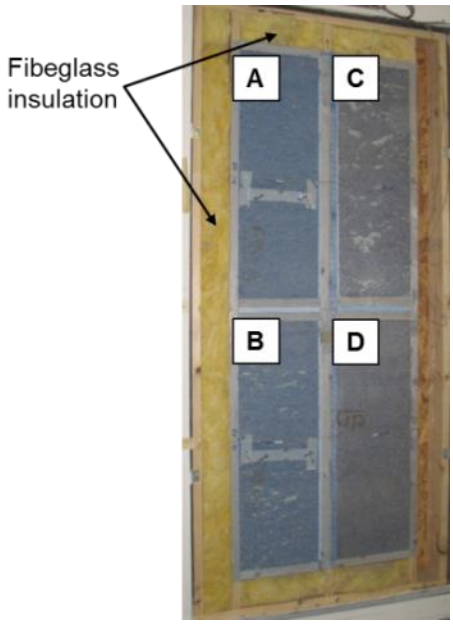

Figure 5. Modified test wall – (A) cellulose-only insulation, (B) cellulose-HDPE mix, (C) cellulose-PCM mix, and (D) cellulose-PCM-cellulose sandwich structure.

Figure 6. Finished interior (left) and exterior (right) sides of the test wall (June 2012).

3. DATA ACQUISITION SYSTEM AND INSTRUMENTATION

Figure 7 shows a typical instrumentation layout in the wall cavities. The wall contained vinyl siding and a weather barrier over OSB on the exterior side of the wall, which is exposed to the atmosphere (as seen on the south wall in Figure 1). The interior side is covered with a gypsum board. Each cavity contains a thermistor and RH sensor combination (T/RH sensor) on the OSB and gypsum surfaces facing the cavity, thermistor inside the cavity (mid-depth) and on the

gypsum surface facing the room interior, and a heat flux transducers on the gypsum surface facing the cavity. Within each cavity, these sensors are located approximately in a line along both the vertical and horizontal midpoints of the cavity. In addition, a single thermistor is attached to the wall exterior (interior face of the siding) and a T/RH sensor combination on the OSB surface facing the exterior, which are not shown in Figure 7. The T/RH sensor is indicated by the white packets seen in Figure 7.

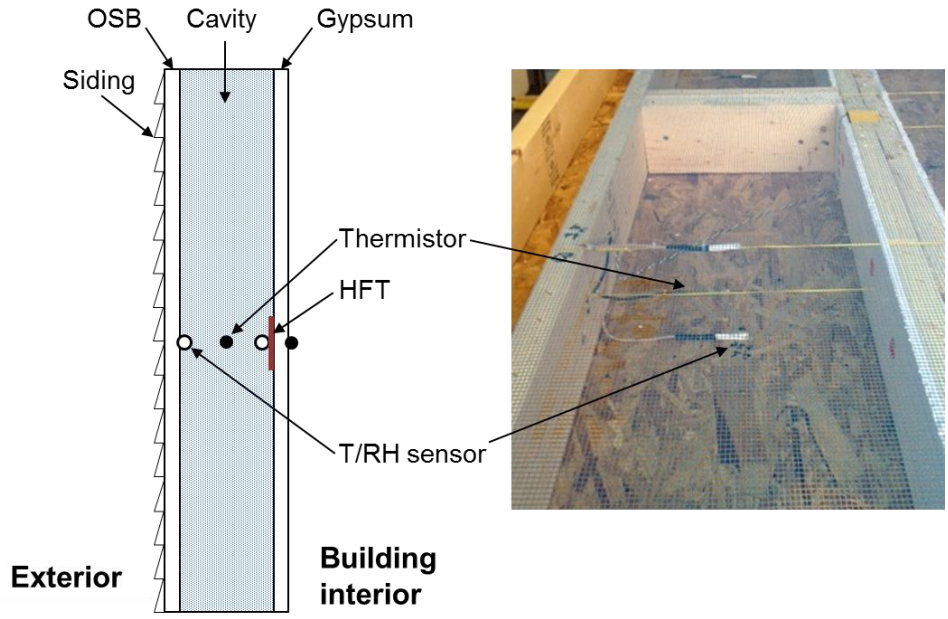

Figure 7. Sensor placement in test wall.

In addition to the sensors attached to the test wall, the NET facility includes sensors and instruments to monitor the local weather conditions, including temperature, humidity, solar irradiance, wind conditions, etc. These sensors are controlled and monitored by Campbell Scientific (CSI) CR10X dataloggers and multiplexers (http://www.campbellsci.com/cr10x). Each sensor is scanned at five minute intervals and the data are then averaged and stored at hourly intervals. The data are downloaded on a weekly basis at ORNL using a dedicated computer and modem. Table 1 provides the sensor list for the NET facility. Table 2 provides the sensor specifications.

Table 1. Charleston NET facility sensor list.

Sensor	Location	Number
Outdoor temperature	Top of building exterior	1
Outdoor RH	Top of building exterior	1
Solar horizontal	Top of building exterior	1
Solar vertical	South center building exterior	1
Wind speed	Top of building exterior	1
Wind direction	Top of building exterior	1
Rainfall horizontal	Top of building exterior	1
Rainfall vertical south 1	South wall center	1
Rainfall vertical south 2	South wall east	1

Rainfall vertical north	North wall east	1
Indoor temperature Rm. 1	Room 1 high and low	2
Indoor RH Rm. 1	Room 1 high and low	2
Indoor temperature Rm. 2	Room 2 high and low	2
Indoor RH Rm. 2	Room 2 high and low	2
Test wall panel thermistors	17 per wall, 18 walls	306
Test wall panel RH sensors	6 per wall, 18 walls	108
Test wall panel moisture pin sets	8 per wall, 18 walls	144

Table 2. Installed sensor accuracy.

Sensor	Accuracy	Sensitivity	Repeatability	Supply Voltage
Fenwall Uni-curve 10K ohm thermistor	± 0.2%	-	± 0.2%	2.5Vdc
Honeywell Hy-Cal Humidity Sensor *HIH-4000 Series*	± 3.5%	-	± 0.5%	5Vdc
Heat Flux Transducer (Concept Engineering Model F-002-4)	± 5%	(5.7 W/m^2)/mV / [(1.8 $Btu/hr\text{-}ft^2$)/mV]	-	-
Outdoor RH (Vaisala CS500)	± 3%	-	-	12Vdc
Wind Speed (R. M. Young Model 05305 Wind Monitor)	± 0.4%	-	-	-
Wind Direction (R. M. Young Model 05305 Wind Monitor)	± 3°	-	-	12Vdc
Rainfall (Texas Electronics Model TE525)	± 1% @ 1”/hr	-	-	-
Solar pyranometer, vertical (LI-Cor LI200X	± 3%	$0.2 \cdot kW \cdot m^{-2} \cdot mV^{-1}$	-	-
Solar pyranometer, horizontal (Kipp & Zonen SP-Lite	± 3%	$10\mu V \cdot W^{-1} \cdot m^{-2}$	-	-
Campbell Sci CR10X w/32 Channel multiplexer	± 0.1% of FSR**	-	-	12Vdc

*MC – Moisture content, **FSR – Full scale reading

4. RESULTS AND DISCUSSION

4.1. Field Data Analysis

This section shows some sample temperature, humidity and heat flux data, with the focus on some key findings. As mentioned earlier, all sensor data have been provided to the sponsor for further detailed analysis and modeling. The intent of this report is not to investigate the overall energy savings, but to examine how the PCM impacts the test wall based on the field data. For the sake of analysis, the monitoring period has been divided into two phases. Phase 1 defines the period before the wall modification took place, from January to June 2012, and phase 2 is the period after June 2012. The data monitoring started around January 18, 2012, and since then they have been compiled into weekly files containing hourly data.

Temperature and Heat Flux

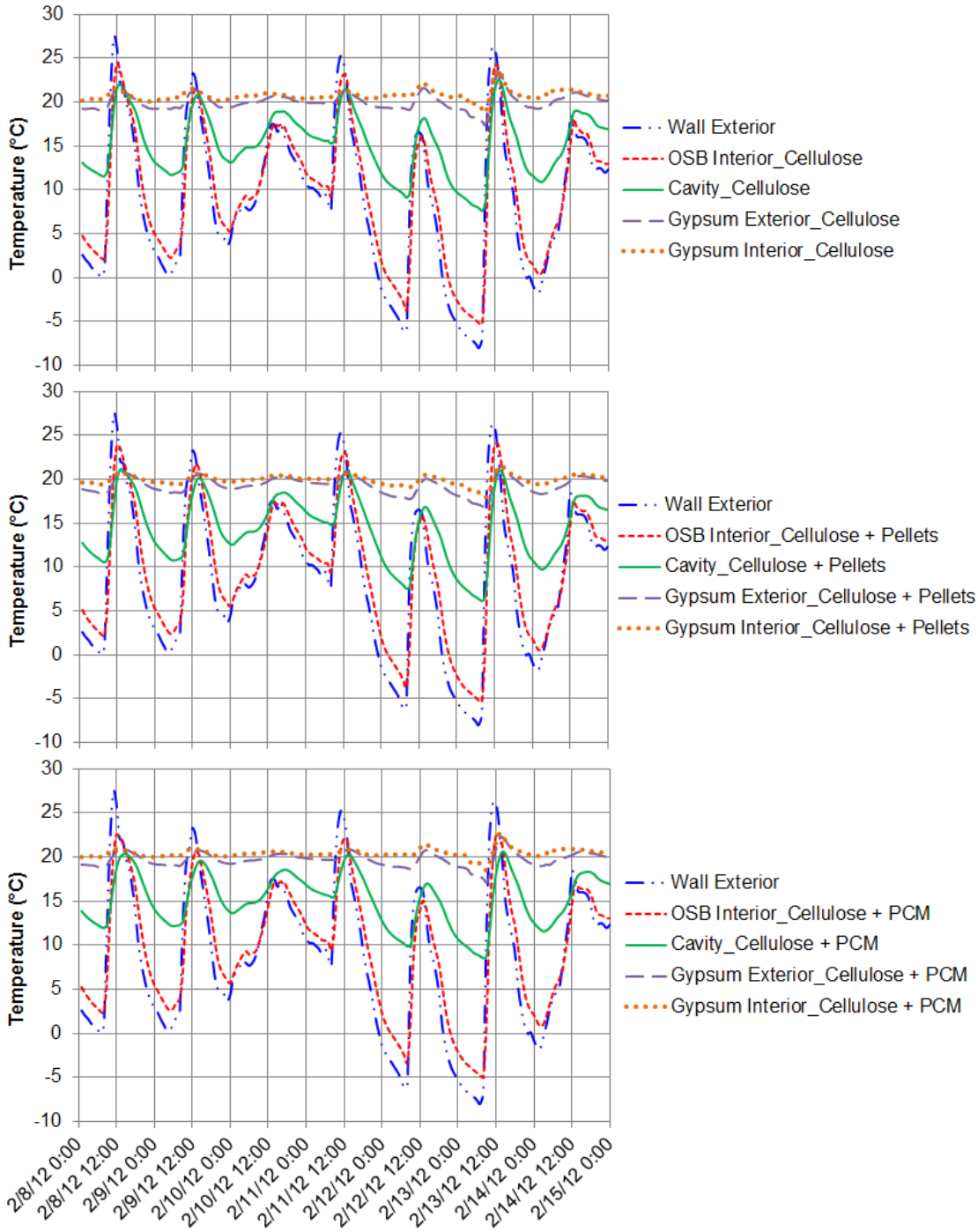

Figure 8. Temperature variations within different wall sections during a phase 1 winter week.

Figure 8 shows the temperature distribution across the wall depth or thickness within the different wall sections ('Cellulose', 'Cellulose + Pellets' and 'Cellulose + PCM') during a winter week in phase 1. This week was chosen since it saw the coldest outside air temperatures during the phase 1 evaluation period. The sensor descriptions are based on their locations within the

test wall. 'Interior' refers to any surface faced towards the building interior and 'Exterior' indicates any surface facing outside to the building exterior. In Figure 8, the 'Wall Exterior' is the thermistor located under the outer vinyl siding, 'OSB Interior' is the thermistor (T/RH combination) on the OSB surface facing the cavity, 'Cavity' is the thermistor installed in the cavity center along its depth, 'Gypsum Exterior' is the thermistor (T/RH combination) facing the cavity (or building exterior), and 'Gypsum Interior' is the thermistor facing the building interior.

As seen in Figure 8, the outer- and innermost surface temperatures were very similar for the different wall sections. Within the cavities, some differences were observed. To further illustrate these differences, the cavity center temperatures from all sections were plotted together and are shown in Figure 9. The data indicate that the cellulose-PCM section showed the least temperature fluctuations in the cavity center.

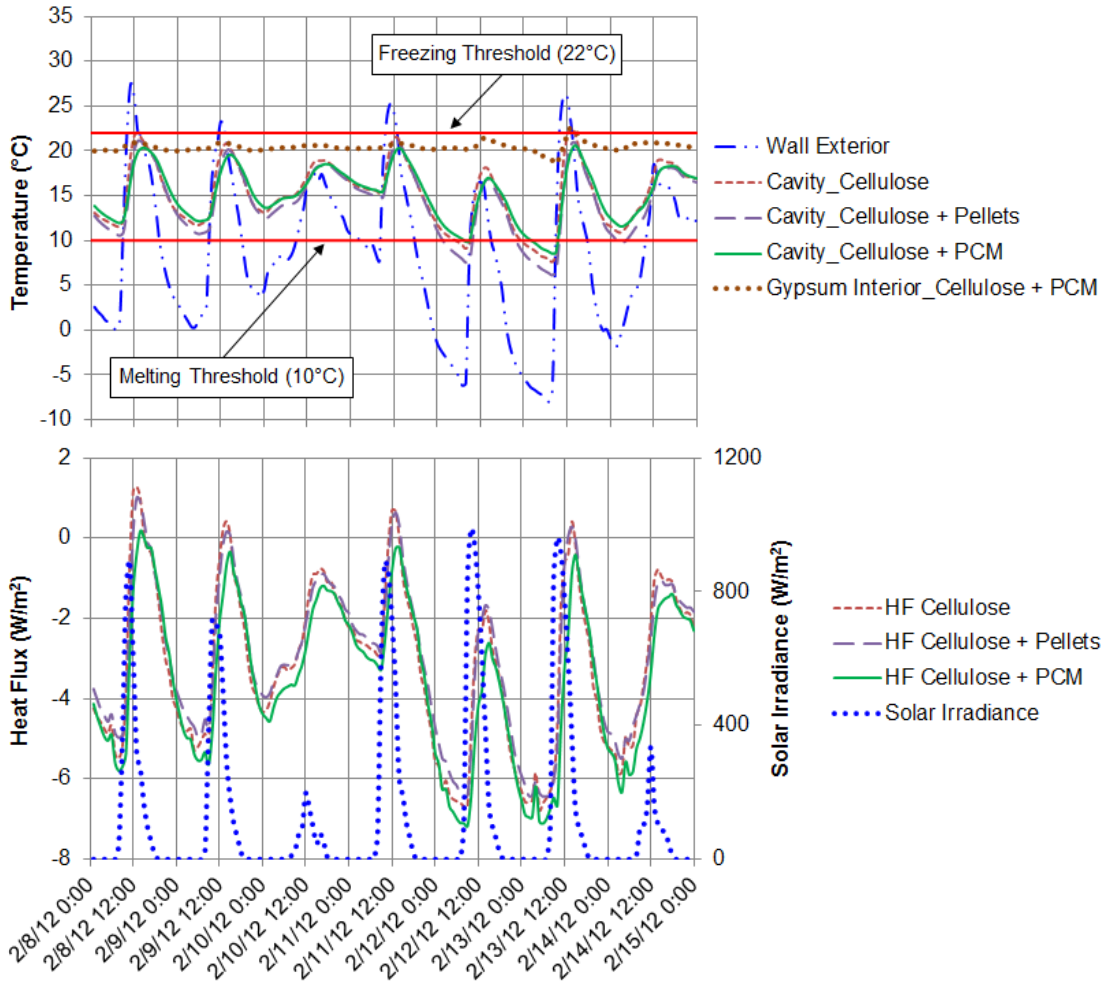

Figure 9. Temperature and heat flux variation for a week during the phase 1 winter period.

To examine whether any phase change was occurring in the PCM section, the threshold temperatures for initiation of melting and freezing have also been included. Melting threshold is the temperature at which the fully frozen PCM will start melting, and at freezing threshold a fully molten PCM will start freezing. The PCM phase change data were obtained using differential scanning calorimetry (DSC) in which the PCM sample were heated or cooled at 1°C

per minute. Further, the DSC measurements revealed that, during heating, the PCM was fully melted at about 38°C. Thus, even during the coldest weather, the PCM was expected to undergo phase change as the PCM cavity and gypsum interior temperatures were always within the phase change temperature range. It should be noted, however, that the DSC heating/cooling rate of 1°C per minute is too high for characterizing PCMs for building applications as the temperature changes in real building envelopes occur at a much slower rate. A different heating/cooling rate can appreciably alter the observed melting and freezing temperature thresholds and ranges [3].

Figure 9 also shows the heat flux variations through the different sections and the south wall solar irradiance (right axis). The heat flux transducers (HFTs) are attached to the exterior surface of the gypsum board (facing the cavity). The sign convention of heat flux is such that heat flow through the gypsum board into the building interior (heat gain) is positive, while heat flow out of the building into the wall cavities (heat loss) is negative. As expected during winter, the heat flow was predominantly out of the building. There was a strong correlation between the daytime heat flux and the solar irradiance. The PCM section showed almost no heat gain during the day and the highest heat loss at night, indicating a negative energy impact during this winter week. The heat fluxes through the 'Cellulose + Pellets' and 'Cellulose' sections were very similar.

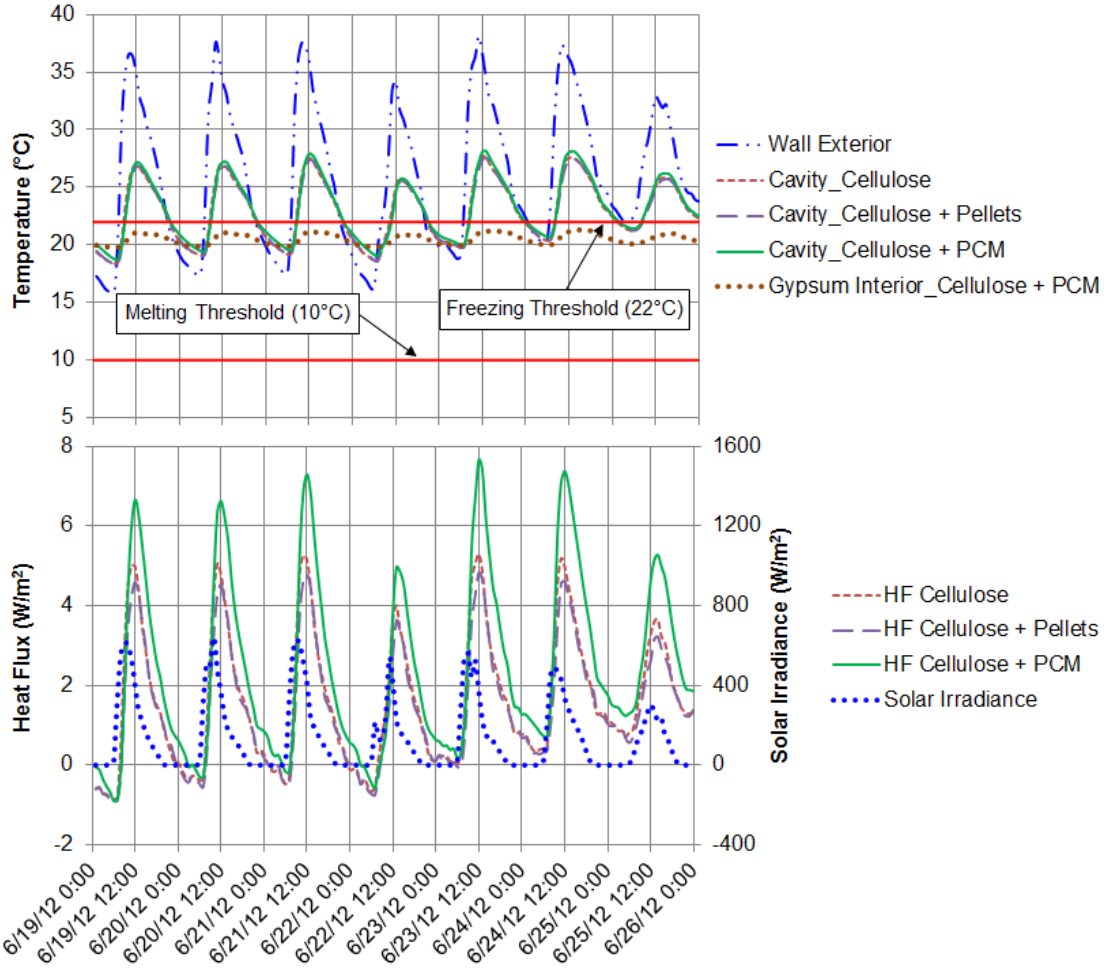

Figure 10. Temperature and heat flux variation for a week during the phase 1 summer period.

Figure 10 shows the cavity center and heat flux comparisons during a phase summer week, with the hottest ambient conditions during phase 1. There were no discernible differences between the cavity center temperatures of the different sections. The cavity center temperatures indicated that the PCM may not be freezing during this period. The heat flux data showed substantially higher heat gains through the cellulose-PCM section, again indicating a negative energy impact compared to cellulose-only insulation. Interestingly, the cellulose-pellets section allowed the lowest peak heat gains.

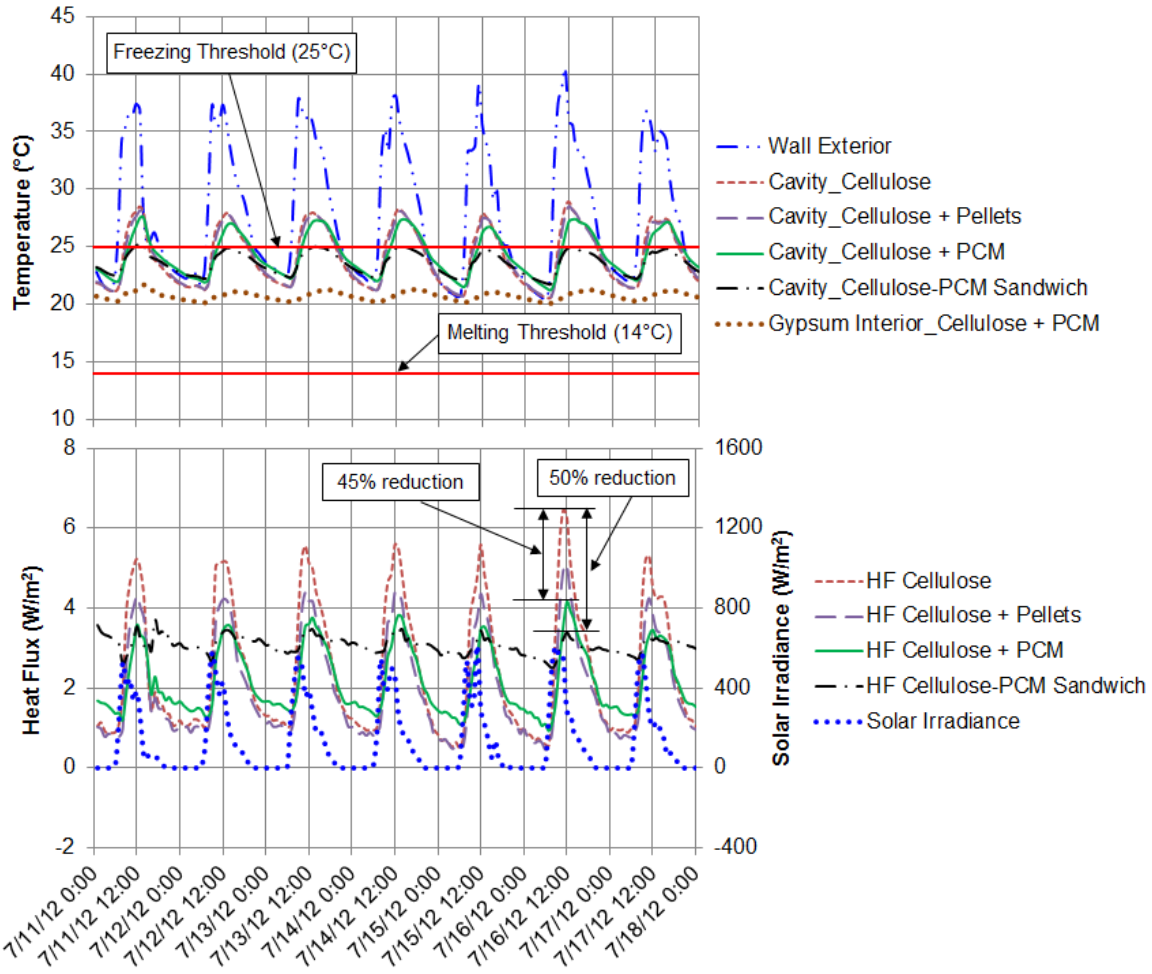

Figure 11. Temperature and heat flux variation for a week during the phase 2 summer period.

On June 27, 2012, the test wall was modified to test another PCM with different phase change characteristics, higher melting and freezing thresholds than the phase 1 PCM. Figure 11 shows the temperature and heat flux data from the four sections during a summer week, when the hottest ambient conditions for the phase 2 period were observed. Again, the cavity center temperatures are relatively high, but with a higher freezing threshold, some phase change can be expected in the cellulose-PCM cavity. The cellulose-PCM sandwich section showed the least fluctuations in the cavity center temperature. With the new PCM, there was a substantial reduction in the peak heat gains, up to 45 and 50% in the cellulose-PCM and cellulose-PCM sandwich sections, respectively, compared to the cellulose-only section. The heat flows were always into the building for all sections, but cellulose and cellulose-pellet sections had lower

heat gains during the nights. This indicates some cooling energy penalty for the PCM containing sections, especially the cellulose-PCM sandwich section.

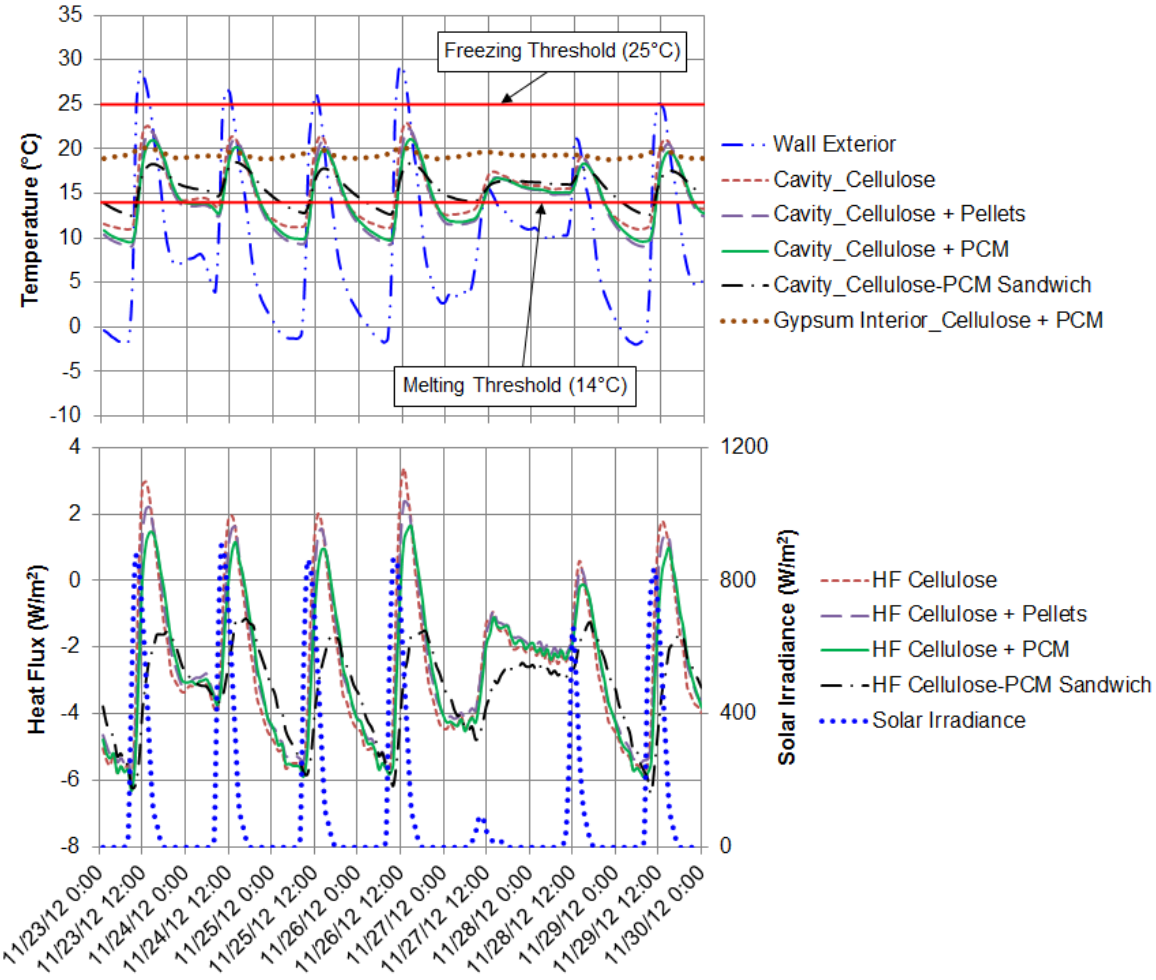

Figure 12. Temperature and heat flux variation for a week during the phase 2 winter period.

Figure 12 shows the temperatures and heat fluxes during a winter week of phase 2. During the week of November 23-30, 2012, the coldest weather for phase 2 was observed. The heat flows were primarily out of the building during this week. There was some daytime heat gain through all sections, except the cellulose-PCM sandwich section. The nighttime losses were similar through all sections. The lower daytime heat gains through the cellulose-PCM section and no heat gains at all through the cellulose-PCM sandwich section indicate heating penalties compared to cellulose-only insulation. It is noted that the coldest period of winter could still be forthcoming and the data collection till end of December will allow better winter performance analysis for the current PCM.

To further investigate the impact of the PCM wall sections, the heat flux data were integrated over 30-day winter and summer periods to determine the total heat gains and losses through the different sections. The integration was performed by a simple application of the trapezoidal rule:

$$Total\ Integrated\ Heat\ Flow\ [\frac{kJ}{m^2}] = \sum_{n=0}^{m} .5 * \Delta X_n * (Y_n + Y_{n+1}) \quad (1)$$

Where Y_n and Y_{n+1} correspond to the current and future time step, ΔX_n is the time step (one hour in this case), and the subscript m denotes the final point in the series which varies depending on the summer or winter data sets. Keep in mind that this integration represents a summation of the area under the curve of the heat flux. The positive and negative heat fluxes were integrated separately to determine the heat gains and losses for each section. The integrated or total heat gains and losses and the net heat transfer during phase 1 (January – June, 2012) are shown in Table 3 and during phase 2 (June – December, 2012) in Table 4. The net heat transfer for each period was obtained by integrating the positive and negative heat fluxes together. Also shown in Table 3 and Table 4 are the percent reductions with respect to the section with only cellulose insulation. The periods considered are listed in the tables, and these were selected based on maximum and minimum 30-day average outside temperatures for the corresponding summer and winter periods, respectively.

During phase 1, the cellulose-PCM section showed a substantial reduction in the heat gained during the winter 30-day period, but showed an increase in the heat lost. Overall, the net transfer was negative for all sections, but the PCM section showed higher losses. During summer, the PCM section showed a large increase in the net heat gain compared to the cellulose-only section. Thus, for the ambient and building conditions, the PCM used during phase 1 had negative energy impacts during both the heating and cooling seasons. The cellulose-pellet section resulted in reduced net heat transfers during both the heating and cooling seasons, compared to the cellulose-only section.

Table 3. Integrated heat flow into and out of the conditioned space through the different cavities during Jan-Jun, 2012.

Cavity	Heat Gain (kJ/m^2)	% Reduction	Heat Loss (kJ/m^2)	% Reduction	Net (kJ/m^2)	% Reduction
Winter 30-day period (Phase 1) (Jan 28 - Feb 26, 2012)						
Cellulose	482.26		-5675.54		-5193.29	
Cellulose + Pellets	387.89	19.57	-5353.36	5.68	-4965.47	4.39
Cellulose + PCM	270.77	43.85	-6180.60	-8.90	-5909.83	-13.80
Summer 30-day period (Phase 1) (May 27 - Jun 25, 2012)						
Cellulose	3635.75		-249.16		3386.59	
Cellulose + Pellets	3265.68	10.18	-262.77	-5.46	3002.91	11.33
Cellulose + PCM	5153.54	-41.75	-171.73	31.07	4981.80	-47.10

During the phase 2 summer period, the cellulose-PCM section reduced the heat gains compared to the cellulose-only section by 12%. While the cellulose-PCM sandwich section was very effective in reducing the peak heat gains (Figure 11), it allowed higher total heat gain compared to the cellulose-only section. During the winter period, the cellulose-PCM section reduced the total heat loss by 4.28%, but also reduced the heat gains by almost 50% compared to the cellulose-only section. The heating penalty due to reduced daytime gains is reflected by a small increase (1.69%) in the net heat loss through the cellulose-PCM compared to the cellulose-only section. The cellulose-PCM sandwich section performed poorly during the winter period, with almost 25% higher total heat loss compared to the cellulose-only section. With the added

thermal mass, the cellulose-pellets section actually performed better than all other wall sections by reducing both heat gains and losses during the summer and winter periods.

Table 4. Integrated heat flow into and out of the conditioned space through the different cavities during Jun-Dec, 2012.

Cavity	Heat Gain (kJ/m^2)	% Reduction	Heat Loss (kJ/m^2)	% Reduction	Net (kJ/m^2)	% Reduction
Summer 30-day period (Phase 2) (Jun 29 - Jul 28, 2012)						
Cellulose	7068.52		0.00		7068.52	
Cellulose + Pellets	5744.47	18.73	0.00		5744.47	18.73
Cellulose + PCM	6218.95	12.02	0.00		6218.95	12.02
Cellulose-PCM Sandwich	8438.94	-19.39	0.00		8438.94	-19.39
Winter 30-day period (Phase 2) (Nov 1 - 30, 2012)						
Cellulose	708.58		-5997.34		-5288.76	
Cellulose + Pellets	535.09	24.48	-5539.69	7.63	-5004.59	5.37
Cellulose + PCM	361.96	48.92	-5740.36	4.28	-5378.40	-1.69
Cellulose-PCM Sandwich	23.22	96.72	-6613.95	-10.28	-6590.73	-24.62

It should be noted that the heat fluxes were local, center-of-cavity values and did not necessarily reflect the energy-savings impact, or lack thereof, of the PCM-enhanced cellulose insulation. Also, the settling of insulation and the stratification of the PCM-containing HDPE pellets added further uncertainty to the local heat flux data (as explained below). It should also be noted that, during phase 1, the cellulose-PCM cavity spanned the entire height of the wall, while the cellulose-only and cellulose-HPDE mix sections were less than half the wall height. There is a potential for uneven settling and density differences in the wall sections, which could potentially impact the heat flows through the center of each section. The local heat flux data are not sufficient to accurately determine the energy-saving impact of the tested PCMs. Detailed energy modeling is required that captures all the building envelope features and indoor and ambient conditions to calculate the annual energy usage to estimate the energy benefits of the cellulose-PCM insulation.

Finally, one source of uncertainties in the measurements needs to be acknowledged. The cellulose-PCM and cellulose-pellets mixing and loading method was such that it was difficult to obtain a uniform distribution of the PCM pellets within the cellulose insulation. Figure 13 shows how the PCM pellets were concentrated in certain regions within the cavities. How the PCM pellets were distributed with respected to the sensors can have an impact on the sensor readings. Figure 14 shows the temperatures measured by three thermistors located mid-depth in the cellulose-PCM cavity along the vertical centerline. The measured temperatures varied by about 5°C (9ºF). depending on the location. Such variability in distribution could also impact the measured heat flows through the sections containing PCM pellets.

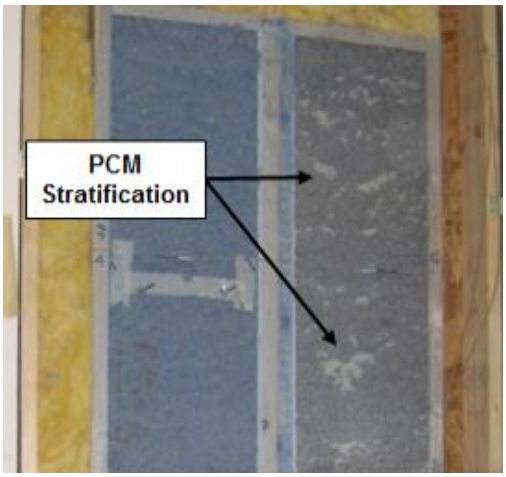

Figure 13. PCM stratification in the cellulose-PCM mixture.

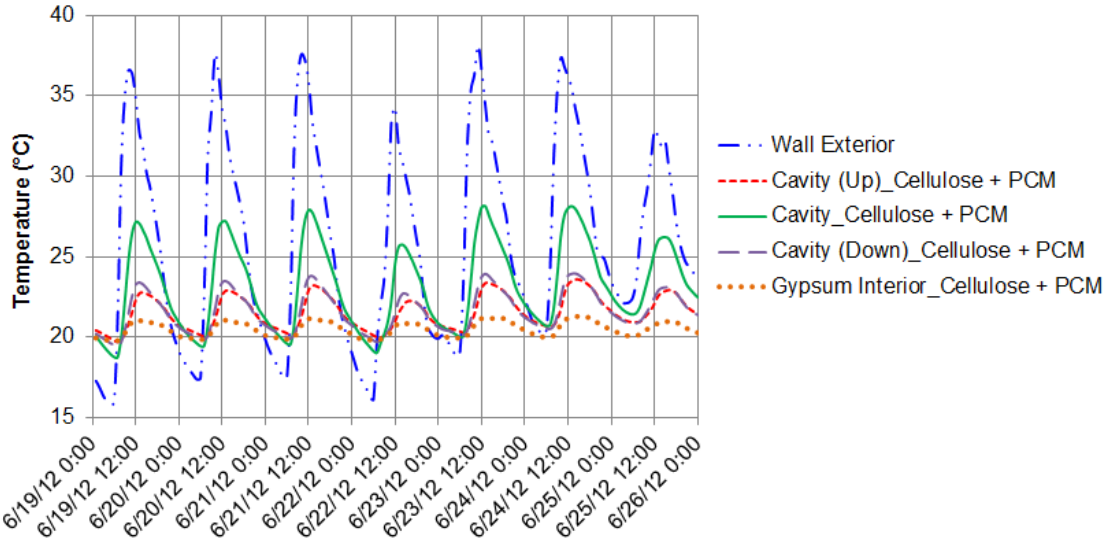

Figure 14. Temperature variation within the PCM containing cavity during phase 1; 'Up' and 'Down' represent locations about 45.7 cm (18 inch) above and below the vertical mid-point of the cavity, and at the centerline along the cavity depth.

Relative Humidity

ASHRAE standard 160 [2] lists the following criteria for minimizing mold growth on the surfaces of building envelope components:

- 30-day running average surface RH < 80% when the 30-day running average surface temperature is between 5°C (41°F) and 37.8°C (100°F)
- 7-day running average surface RH < 98% when the 7-day running average surface temperature is between 5°C (41°F) and 37.8°C (100°F)
- 24-hour running average surface RH < 100% when the 24-hour running average surface temperature is between 5°C (41°F) and 37.8°C (100°F)

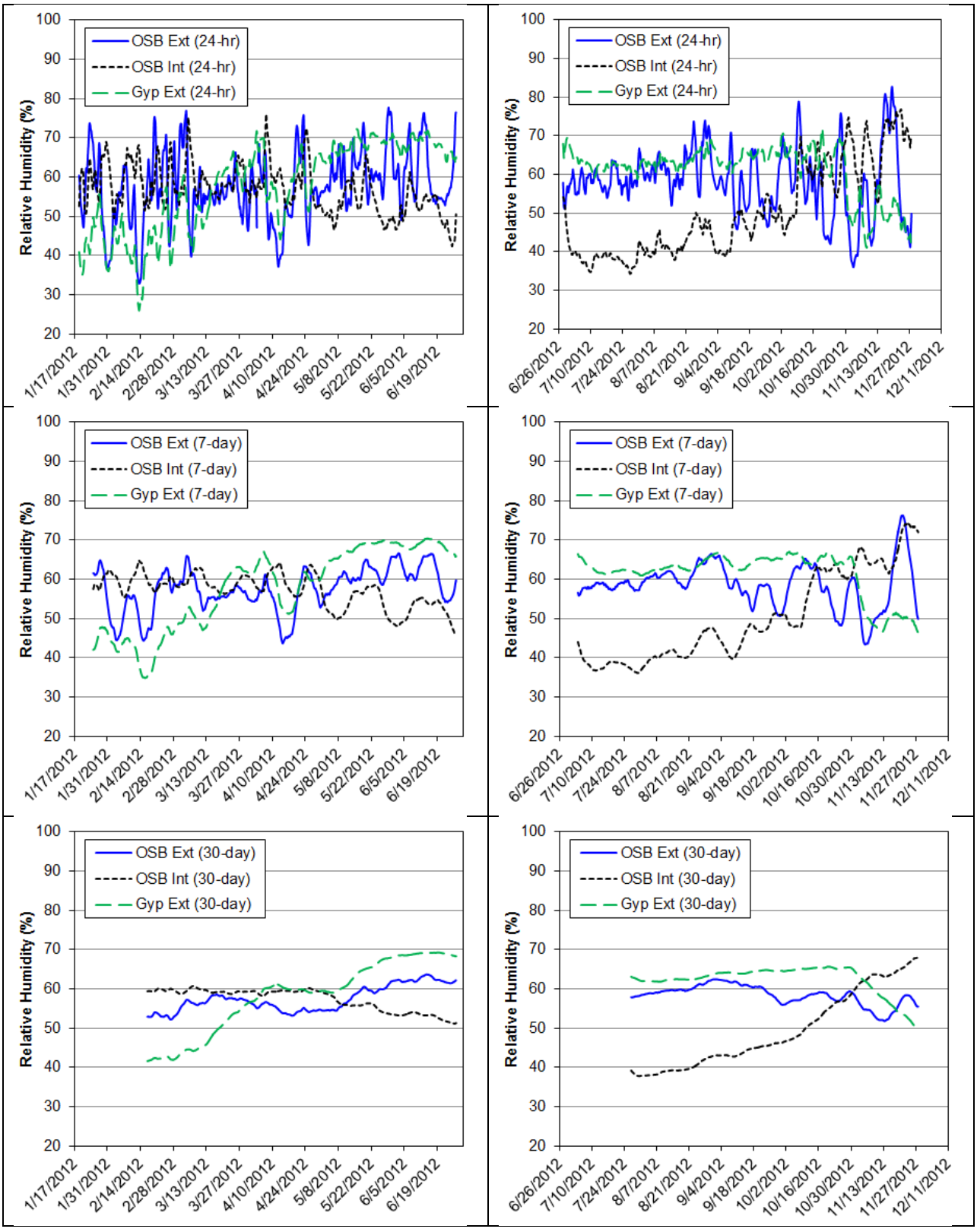

Figure 15. Running averages of relative humidity in different locations on the test wall.

Figure 15 shows the 24-hour, 7-day and 30-day running averages of the surface relative humidity at different locations within the test wall. Each cavity contained a pair of RH sensors, one on the interior face of the OSB ('OSB Int') and the exterior face of the gypsum board ('Gyp Ext'). However, the measurements were nearly identical for the corresponding locations within each cavity. Therefore, for the sake of clarity, only one pair of OSB interior and gypsum exterior RH measurements is shown. The surface temperatures were usually within the 5-37.8°C range, or lower (which would mean lower specific humidity and moisture content). It is evident from Figure 15 that none of the surfaces were ever close to the conditions needed for mold growth.

4.2. Thermal Conductivity Measurements

At the request of the sponsor, in addition to the field test, small test boxes were built and filled with cellulose insulation with and without PCM pellets to test in a heat flow meter apparatus (HFMA) (http://www.lasercomp.com/product/fox6xx.php) according to ASTM C 518 standard test method [4]. A brief description of the HFMA is provided here. The apparatus consists of two plates, upper and lower, which sandwich the test specimen. Each plate is outfitted with solid state heating/cooling systems, and the two specimen surface temperatures can be independently controlled to induce heat flow in either upward or downward direction through the specimen. Thin film heat flux transducers (HFTs) are permanently bonded to the upper and lower plate surfaces. The HFTs are of integrating type, with a 20.3 x 20.3 cm^2 (8 x 8 $inch^2$) active area in the center of each plate. In the center of the each transducer, a thermocouple is bonded near its surface, close to the test specimen. These thermocouples accurately measure the specimen surface temperatures and are also used to control the plate temperatures. Figure 16 shows the apparatus used for the thermal conductivity measurements.

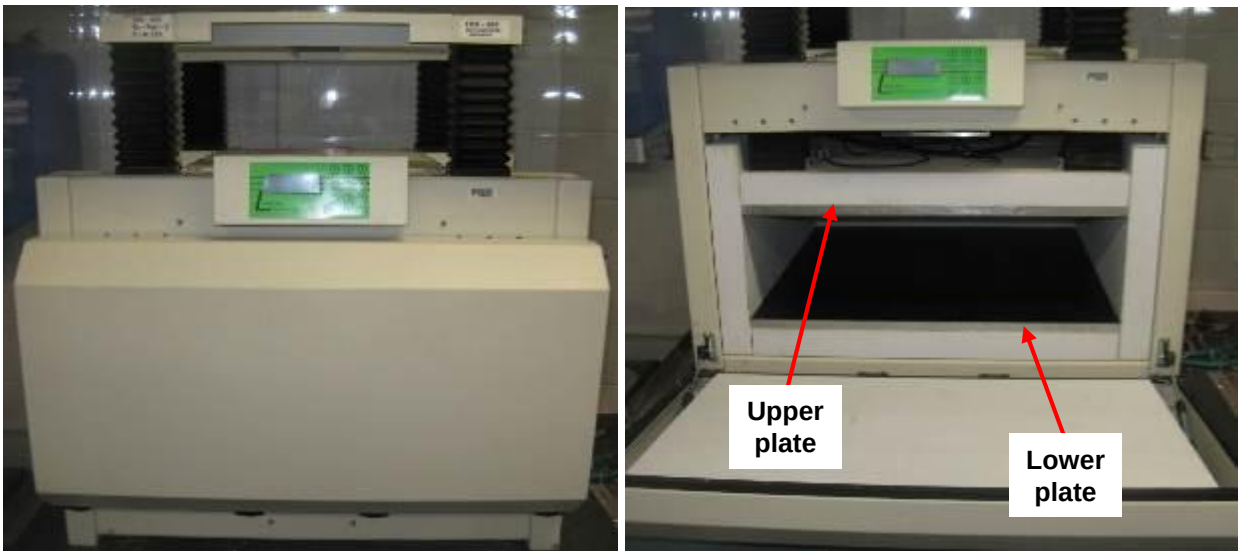

Figure 16. Heat flow meter apparatus.

During tests, a set of data is taken once every 0.7 seconds. Each set of data includes the upper and lower plate temperatures and heat flux transducer outputs. 512 consecutive sets of data are organized in one block and are averaged to yield the mean plate temperatures and heat fluxes. The following three equilibrium criteria were used to determine the completion of the tests:

1. Temperature equilibrium: The block average temperature of each plate must be within 0.2ºC of the previous block.
2. Semi-equilibrium: The average heat flux transducer output of a block must be within 70 microvolts (μV) of the previous block's average.
3. Percent-equilibrium: The average block heat flux transducer output of a block must be within a 2% of the previous block's average.

An additional criterion for test completion is the absence of any monotonic trends in the test data. Once a certain number of consecutive blocks, minimum of 30 for the present tests, satisfied all equilibrium criteria, the test for a given temperature set point is completed. With the measured sample thickness, upper and lower plate temperatures and heat fluxes, the thermal conductivity of the test specimen can be calculated. For calculating the result, the last 5 blocks out of the consecutive blocks that satisfied the equilibrium criteria were used.

Figure 17 shows the test box that was filled with cellulose mixed with 20% by weight PCM (phase 1). The cellulose and PCM were from the same batches that were used in the Charleston test wall. The filling mixing and filling mechanism was also the same as the Charleston test walls. The interior box dimensions were 55.9 x 56.5 x 14.0 cm^3 (22 x 22.3 x 5.5 $inch^3$) and the resulting density of the cellulose-PCM mix was 56.6 kg/m^3 (3.5 lb/ft^3) after filling. The test box contained an OSB on one side and a net on the other, to contain the insulation. This box was tested twice, once after two days and then after another month. During this time, the test box was placed in an un-insulated test attic at ORNL to allow the PCM to undergo several phase change cycles. Before both tests, it was observed that the top of the test box showed a gap due to settling of the insulation, similar to the Charleston test wall. It needed to be filled with insulation to prevent convection cells forming in the air gap while being tested in the HFMA. With the added insulation, the resulting densities were 62.5 kg/m^3 (3.9 lb/ft^3) and 70.4 kg/m^3 (4.4 lb/ft^3). The test box was tested with the OSB resting on the lower plate.

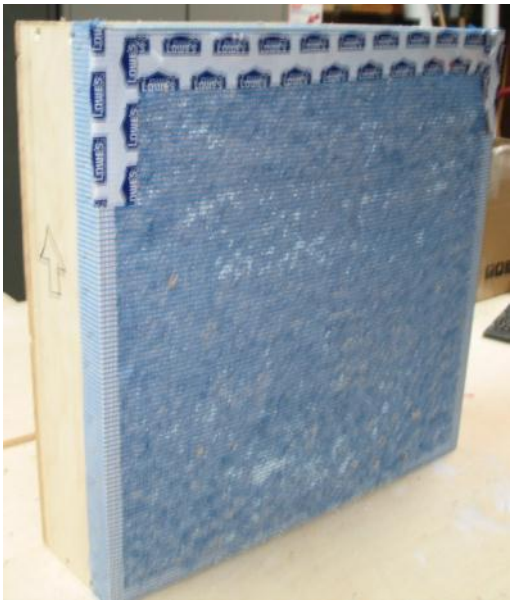

Figure 17. Test box used for the thermal conductivity measurements.

For reference, a second test box was built and filled with only cellulose insulation. The box cavity dimensions were 55.6 x 55.6 x 14.0 cm^3 (21.9 x 21.9 x 5.5 $inch^3$) and the filled density of cellulose was 42.4 kg/m^3 (1.5 lb/ft^3). The test box samples were tested at two different sets of HFMA plate temperatures, 0 and 15°C and 40 and 55°C. Given the temperature limits of the HFMA, the temperatures were chosen so that they were above and below the PCM phase change temperature range to the extent possible. Table 5 summarizes the measured thermal conductivities of the test boxes. The 'unaged' PCM refers to the test conducted 2 days after preparing the sample and 'aged' refers to the test conducted after 30-plus days.

Table 5. Summary of thermal conductivity measurements.

	Upper Temp (°C)	Lower Temp (°C)	Mean Temp (°C)	Upper Cond (W/mK)	Lower Cond (W/mK)	Average Cond (W/mK)
Cellulose only	0.01	15.01	7.51	0.04416	0.03576	0.03996
	40.02	55.02	47.52	0.04796	0.04979	0.04887
Unaged PCM + Cellulose	0.01	15.01	7.51	0.04827	0.03122	0.03974
	40.02	55.02	47.52	0.04715	0.05782	0.05248
Aged PCM + Cellulose	0.01	15.01	7.51	0.04734	0.04091	0.04413
	40.03	55.02	47.52	0.04552	0.05824	0.05188

As indicated by the difference in the upper and lower conductivities (determined using the HFTs in the upper and lower plates, respectively), especially at the lower temperature range, there were two-dimensional heat transfer effects present (i.e. edge losses through the framing of the test boxes). There are additional uncertainties in the test data due to the settling of cellulose and stratification of the PCM in the box with the PCM-cellulose mix. According to the HFMA specifications, the instrument has an accuracy better than 1%, with 0.2% repeatability and 0.5% reproducibility. The tests were set to continue for a minimum number of 30 block (~180 minutes) once all equilibrium criteria were met, with the final 5 blocks used for calculating the thermal conductivities. The PCM-cellulose tests ran for a minimum of 16 hours, while the cellulose-only tests ran for a minimum of 8 hours.

5. SUMMARY

A field test of a low-cost PCM is currently ongoing in a natural exposure test facility in Charleston, SC. Temperature and heat flow data from the test wall sections with different combinations of cellulose-PCM-HDPE pellets were analyzed and the main findings are presented in this report. The PCM installed in the test walls showed potential for energy savings, compared to conventional cellulose insulation. The data have been provided to the sponsor for further analysis and energy modeling, which are needed to quantify the actual energy savings with the PCM-enhanced insulation for different building and climate types. Interestingly, the addition of HDPE pellets (without PCM) also showed improved thermal performance compared to cellulose-only insulation.

6. REFERENCES

1. Kosny, J., Yarbrough, D. W., Miller, W. A., 2007. “Use of PCM Enhanced Insulation in the Building Envelope,” Oak Ridge National Laboratory, Oak Ridge, TN.
2. ANSI/ASHRAE Standard 160-2009, Criteria for Moisture-Control Design Analysis in Buildings, 2009.
3. Kosny, J., Biswas, K., Miller, W., Kriner, S., 2012. “Field Thermal Performance of Naturally Ventilated Solar Roof with PCM Heat Sink,” Solar Energy, v 86, n 9, p 2504-2514.
4. ASTM C518-04: Standard Test Method for Steady-State Thermal Transmission Properties by Means of the Heat Flow Meter Apparatus.